Filtered Split-Path Nonlinear Integrator (F-SPANI) for improved transient performance

Maas, A; Van De Wouw, N.; Heemels, W. P Maurice H

DOI
10.23919/ACC.2017.7963488

Publication date
2017

Document Version
Final published version

Published in
Proceedings 2017 American Control Conference (ACC 2017)

2017 American Control Conference
Sheraton Seattle Hotel
May 24–26, 2017, Seattle, USA

Filtered Split-Path Nonlinear Integrator (F-SPANI) for improved transient performance

A. van der Maas, N. van de Wouw, W.P.M.H. Heemels

Abstract— **The recently introduced Split-Path Nonlinear Integrator (SPANI) is designed to improve the transient performance of linear (motion) systems in terms of overshoot. The SPANI was shown to be an effective nonlinear controller to improve transient performance by enforcing the same sign in the integrator action and the error. However, to avoid (fast) switching in the control input in steady-state, conservatism had to be introduced in the SPANI design, thereby limiting the performance. In this paper, this conservatism is removed by introducing a new design, called the Filtered Split-Path Nonlinear Integrator (F-SPANI). This design is based on the inclusion of an additional filter in the phase path, which enables the full potential behind the main idea of the SPANI. The ease of the design and implementation and the potential of the proposed controller are illustrated both in simulation and in experiments on a motion system.**

I. INTRODUCTION

The Bode gain-phase relationship reveals a hard limitation on the achievable transient performance using classical linear controllers, see, e.g., [1], [2]. As a result, a trade-off exists between (transient) performance and disturbance suppression in linear time-invariant (LTI) feedback control [3]. A typical example is the use of an integrator in feedback control, which results in a zero steady-state error at the cost of overshoot due to the 90 degrees phase lag of the integrator, which serves as a buffer.

Since the Bode gain-phase relation is a widely known limitation for *linear* control techniques, nonlinear and hybrid control strategies have been designed to improve (amongst others) the transient performance of LTI systems, see, e.g., [4]. Reset control is a typical example, where (a subset of) the states are reset if certain conditions are met to reduce the overshoot, see, e.g., the Clegg integrator [5]. Over the last two decades, reset control strategies have regained the attention, both in research, [6], [7], [8], and in applications, [9]. Other examples to improve transient performance are, amongst others, variable-gain integrators [10], [11], and sliding mode controllers with saturated integrators [12].

This research is supported by the Dutch Technology Foundation STW, carried out as part of the CHAMeleon project "Hybrid solutions for cost-aware high-performance motion control" (no. 13896).

N. van de Wouw is with the Department of Mechanical Engineering, Eindhoven University of Technology, Eindhoven 5600 MB, The Netherlands, with the Department of Civil, Environmental and Geo-Engineering, University of Minnesota, Minneapolis, MN 55455 USA, and also with the Delft Center for Systems and Control, Delft University of Technology, Delft 2628 CD, The Netherlands (e-mail: n.v.d.wouw@tue.nl).

A. van der Maas and W.P.M.H. Heemels are with the Department of Mechanical Engineering, Control Systems Technology group, Eindhoven University of Technology, 5600 MB Eindhoven, The Netherlands (e-mail: {a.v.d.maas, m.heemels}@tue.nl)

In this paper, we are interested in the line of nonlinear controllers based on the Split-Path Nonlinear (SPAN) filter, which has been introduced in [13] and facilitates independent tuning of the phase and the amplitude characteristics. In [14], the so-called Split-Path Nonlinear Integrator (SPANI) is proposed by adopting an integrator in the SPAN filter. The main benefit of the SPANI in [14] is the combination of an increased transient performance and the ease of verification of stability of the switching closed-loop system. The SPANI is easily tunable using the standard tools for controller design based on, for instance, loop-shaping, enabling straightforward adoption in industrial practice. In fact, without complex optimizations, the transient performance can be improved significantly. The SPANI switches the sign of the integrator depending on the sign of the tracking error of the feedback loop. Since the system is in equilibrium for a zero error, any slight disturbance will cause the controller to switch. To avoid the undesirable switching while the system already reached the final position, the switching rule was changed to include the equilibrium in the interior of the region corresponding to one of the modes of the switched system, which causes a slight phase lag. The drawback of this changed switching rule is that the SPANI does not reach the full potential for performance improvement, since the phase lag results in delayed switching compared to the SPANI, which in turn induces a larger overshoot.

The purpose of this paper is to overcome the conservatism in the SPANI by introducing a *Filtered Split-Path Nonlinear Integrator* (F-SPANI) as a novel hybrid controller. The F-SPANI extends the SPANI structure by introducing a well-designed filter in the phase path. It is shown that addition of a filter providing a phase lead, such as a lead filter, results in a significant improvement in transient performance. Moreover, it is shown that the stability analysis of the SPANI remains valid for the F-SPANI. The potential benefits of the novel F-SPANI design are shown in both simulations and experiments on a motion system, thereby also illustrating the ease of the design. For both the SPANI and the F-SPANI, the experimental validation has never been shown before.

In Sec. II, the SPANI of [14] is briefly recalled. In particular, a sketch of the stability proof is given in Sec. II-B, and the main limitation of the SPANI is highlighted in Sec. II-C. In Sec. III, the filtered SPANI is introduced, and it is shown that the stability analysis from II-B can be extended to the F-SPANI. In Sec. IV, the benefits of the proposed approach are shown in simulations. In Sec. V, measurement results are shown for an experimental motion system. In Sec. VI, the conclusions of the paper are given.

978-1-5090-5992-8/$31.00 ©2017 AACC

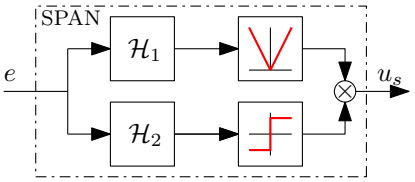

Fig. 1: Block diagram of the SPAN filter.

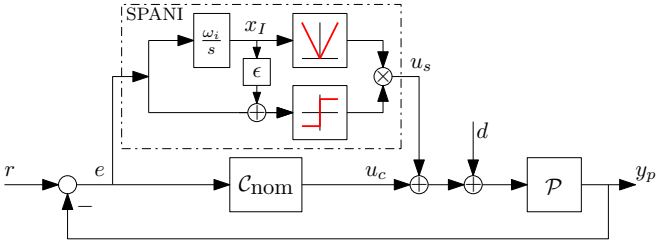

Fig. 2: Closed-loop SPANI with tilting parameter ϵ.

II. SPLIT-PATH NONLINEAR INTEGRATOR

A. Description of the SPANI

The original idea behind the SPAN filter [13], as shown in Fig. 1, is to separately tune the amplitude and phase in the controller design. The SPANI and the proposed filtered SPANI (F-SPANI) are specific cases of the SPAN filter. In general, the SPAN filter is schematically represented as in Fig. 1, where $\mathcal{H}_1$ and $\mathcal{H}_2$ can be chosen to be any filter. In the SPANI, $\mathcal{H}_1$ is selected to be an integrator and $\mathcal{H}_2$ as a gain of 1. By combining this with a nominal controller $\mathcal{C}_{\text{nom}}$, the full control structure results as in Fig. 2 for $\epsilon = 0$. The SPANI results in a switched system, where the integrator action u_s has the same sign as the error e at any time. It can be written in state-space form as

$$\text{SPANI}: \begin{cases} \dot{x}_I &= \omega_i e, \\ u_s &= \begin{cases} +x_I & \text{if} \quad ex_I \geq 0, \\ -x_I & \text{if} \quad ex_I < 0, \end{cases} \end{cases} \tag{1}$$

with $x_I \in \mathbb{R}$ the integrator state and u_s the output of the SPANI. The other system dynamics in Fig. 2 can also be written in state-space form. Hereto, let the plant be defined by

$$\mathcal{P}: \begin{cases} \dot{x}_p &= A_p x_p + B_p u + B_p d \\ y_p &= C_p x_p \end{cases} \tag{2}$$

with state $x_p \in \mathbb{R}^{n_p}$, $u = u_c + u_s \in \mathbb{R}$ the total control input of the system $\mathcal{P}$, $d \in \mathbb{R}$ the disturbance, and $y_p \in \mathbb{R}$ the output. The nominal LTI controller for this system is given by

$$\mathcal{C}_{\text{nom}}: \begin{cases} \dot{x}_c &= A_c x_c + B_c e, \\ u_c &= C_c x_c + D_c e, \end{cases} \tag{3}$$

where $e = r - y_p \in \mathbb{R}$ is the error of the feedback loop, $x_c \in \mathbb{R}^{n_c}$ the state of the controller and $u_c \in \mathbb{R}$ the output of the nominal controller.

The overall closed-loop system is now given by

$$\dot{x} = \begin{cases} A_1 x + B_r r + B_d d \quad \text{if} \quad ex_I \geq 0, & \text{(4a)} \\ A_2 x + B_r r + B_d d \quad \text{if} \quad ex_I < 0 & \text{(4b)} \end{cases}$$

where A_1, A_2, B_r, and B_d can directly be derived from (1)-(3), with $x = \begin{bmatrix} x_p^\top & x_c^\top & x_I \end{bmatrix}^\top$. The linear parts of the controller, i.e., $\mathcal{C}_{\text{nom}}(s)$ and $\mathcal{C}_{\text{I}}(s) = \frac{\omega_i}{s}$, define the dynamics in (4a), i.e., for $x_I e > 0$. Here, it is assumed that the user-designed closed-loop dynamics are asymptotically stable, such that the eigenvalues of A_1 have all a strictly negative real part, i.e., A_1 is Hurwitz. Due to a minus-sign in A_2, it typically holds that mode 2 in (4b) is unstable. The output of the total system is identical to the output of the open-loop plant $\mathcal{P}$, i.e., $y_p = C_p x_p = \begin{bmatrix} C_p & O_{1\times n_c} & 0 \end{bmatrix} x$.

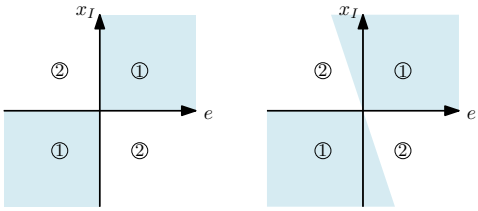

(a) $\varphi = ex_I$ (b) $\varphi = x_I(x_I\epsilon + e)$

Fig. 3: (e, x_I)-plane with and without tilting parameter ϵ. In mode 1, $\varphi > 0$; in mode 2, $\varphi < 0$.

The equilibrium state for a constant reference r_c and constant disturbance d_c satisfies

$$x^* = -A_1^{-1}\left(B_r r_c + B_d d_c\right), \tag{5}$$

where x^* represents the equilibrium state, which corresponds to $e = 0$ according to (1). This equilibrium introduces a non steady-state control effort, even though the system is in steady-state. The (e, x_I)-plane is shown in Fig. 3a, and is a valuable tool in understanding the working principle of the SPANI. This figure shows that the projected equilibrium point $(e^*, x_I^*) = (0, x_I^*)$ is located exactly at the switching boundary $\varphi := ex_I = 0$. Due to the position of the equilibrium point, any deviation from $e = 0$ will cause the SPANI output u_s to switch sign, see (1). Switching at $e = 0$ is undesired since it causes oscillatory behavior around the equilibrium, see [14] for more details.

To avoid such switching around an equilibrium, the switching rule in [14] was changed to include a tilting parameter ϵ, resulting in the extended SPANI

$$\text{SPANI}: \begin{cases} \dot{x}_I &= \omega_i e, \\ u_s &= \begin{cases} +x_I & \text{if} \quad x_I(\epsilon x_I + e) \geq 0, \\ -x_I & \text{if} \quad x_I(\epsilon x_I + e) < 0. \end{cases} \end{cases} \tag{6}$$

The effect of the tilting parameter is schematically shown in the (e, x_I)-plane in Fig. 3b. Using the tilting parameter, the full model of the SPANI changes to

$$\dot{x} = \begin{cases} A_1 x + B_r r + B_d d \quad \text{if} \quad x_I(\epsilon x_I + e) \geq 0, & \text{(7a)} \\ A_2 x + B_r r + B_d d \quad \text{if} \quad x_I(\epsilon x_I + e) < 0. & \text{(7b)} \end{cases}$$

The inclusion of the tilting parameter guarantees that the equilibrium x^* corresponding to $e = 0$ always lies in the stable mode 1, as defined in (7a). In Sec. II-B, a sketch of the stability proof of the SPANI is provided.

B. Stability

In [15], the stability proof for the overall closed-loop system as described by (7) is given. In this section, a sketch of the proof is given, since one of the contributions of this

paper is to show that the stability of the F-SPANI can be checked using similar tools as in the case of the SPANI. The first step in the stability proof is to perform a coordinate transformation around the equilibrium point, i.e., $\tilde{x} = x - x^*$, where x^* is defined by (5). In terms of the new coordinates $\tilde{x}$, a quadratic Lyapunov function $V(\tilde{x}) = \tilde{x}^\top P \tilde{x}$ will be used with positive definite matrix P.

The stability of the SPANI can then be checked by guaranteeing the decay of the Lyapunov function for three regions, i.e., for $\varphi > 0$ (mode 1), for $\varphi < 0$ (mode 2), and for $\varphi = 0$ (including the case of a possible sliding mode at the switching boundary). To facilitate the notation, the switching boundary can be written as

$$\varphi = x_I(\epsilon x_I + e) = \tilde{x}_a^\top R \tilde{x}_a = 0 \tag{8}$$

with augmented states $\tilde{x}_a = \begin{bmatrix} \tilde{x}^\top & r_c & d_c \end{bmatrix}^\top$ and the symmetric matrix

$$R = \begin{bmatrix} O_{n_p \times n_p} & O_{n_p \times n_c} & -\frac{1}{2}C_p^\top & -\frac{1}{2}\gamma_r C_p^\top & -\frac{1}{2}\gamma_d C_p^\top \\ O_{n_c \times n_p} & O_{n_c \times n_c} & O_{n_c \times 1} & O_{n_c \times 1} & O_{n_c \times 1} \\ -\frac{1}{2}C_p & O_{1 \times n_c} & \epsilon & \epsilon\gamma_r & \epsilon\gamma_d \\ -\frac{1}{2}\gamma_r C_p & O_{1 \times n_c} & \epsilon\gamma_r & \epsilon\gamma_r^2 & \epsilon\gamma_r\gamma_d \\ -\frac{1}{2}\gamma_d C_p & O_{1 \times n_c} & \epsilon\gamma_d & \epsilon\gamma_r\gamma_d & \epsilon\gamma_d^2 \end{bmatrix}, \tag{9}$$

where γ_r and γ_d characterize the equilibrium point of the integrator state, i.e., $x_I^* = \gamma_r r_c + \gamma_d d_c$. Based on (5),

$$\gamma_r = -\begin{bmatrix} O_{1 \times n_p} & O_{1 \times n_c} & 1 \end{bmatrix} A_1^{-1} B_r, \tag{10}$$

$$\gamma_d = -\begin{bmatrix} O_{1 \times n_p} & O_{1 \times n_c} & 1 \end{bmatrix} A_1^{-1} B_d. \tag{11}$$

To guarantee stability, the time derivative of the Lyapunov function should be strictly negative for all $\tilde{x} \neq 0$, i.e.,

$$\dot{V}(\tilde{x}) = \begin{cases} \tilde{x}^\top \left(A_1^\top P + P A_1\right) \tilde{x} & \text{if } \tilde{x}_a^\top R \tilde{x}_a > 0, \text{(12a)} \\ \tilde{x}_a^\top Q(P) \tilde{x}_a & \text{if } \tilde{x}_a^\top R \tilde{x}_a < 0, \text{(12b)} \\ \lambda \tilde{x}^\top \left(A_1^\top P + P A_1\right) \tilde{x} & \\ \quad + (1-\lambda) \tilde{x}_a^\top Q(P) \tilde{x}_a & \text{if } \tilde{x}_a^\top R \tilde{x}_a = 0 \text{ (12c)} \end{cases}$$

should be negative for all $\tilde{x} \neq 0$, with

$$Q(P) = \begin{bmatrix} A_2^\top P + P A_2 & P A_d A_1^{-1} B_r & P A_d A_1^{-1} B_d \\ B_r^\top A_1^{-\top} A_d^\top P & 0 & 0 \\ B_d^\top A_1^{-\top} A_d^\top P & 0 & 0 \end{bmatrix}, \tag{13}$$

where $A_d = A_1 - A_2$. In (12c) it holds that $0 \leq \lambda \leq 1$ corresponds to Fillipov's convex definition [16]. It was shown in [14], [15], that, for each of the cases in (12a)-(12c), there exists a $c > 0$ such that for all $\tilde{x} \neq 0$

$$\dot{V}(\tilde{x}) \leq -c \|\tilde{x}\|^2 \tag{14}$$

if there exists an $\alpha \geq 0$ such that the Linear Matrix Inequality (LMI) conditions

$$\begin{cases} A_1^\top P + P A_1 \prec 0, & \text{(15a)} \\ M^\top \left(Q(P) - \alpha R\right) M \prec 0 & \text{(15b)} \end{cases}$$

are satisfied, where

$$M = \begin{bmatrix} I_{n \times n} & O_{n \times 1} \\ O_{2 \times n} & \begin{bmatrix} \gamma_r \\ \gamma_d \end{bmatrix} \end{bmatrix} \tag{16}$$

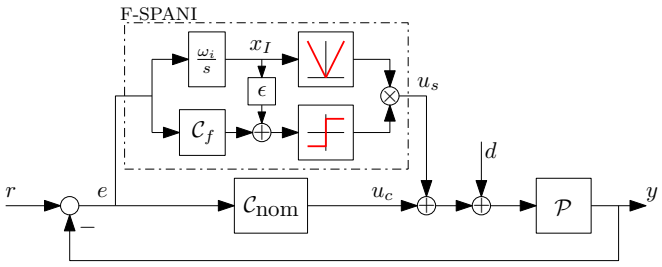

Fig. 4: Closed-loop filtered SPANI.

for $n = n_p + n_c + 1$ the number of states of the complete system.

To guarantee stability for the SPANI, the matrix inequalities in (15) have to be validated, where $\alpha \geq 0$, $P = P^\top \succ 0$ and $\epsilon \geq 0$ are free parameters. It is desired to find the smallest value of ϵ for which the conditions are still met, since this will result in the best transient performance while avoiding oscillatory behavior in the steady-state. The parameters for α and P appear linearly in the matrix inequalities; however, this is not the case for ϵ, and, therefore, an iterative bi-section algorithm is used to find the smallest value for ϵ such that the LMI in α and P is feasible. The smallest value for ϵ is desired to minimize the conservatism of the SPANI, i.e., switch as soon as possible, see [17].

C. Essential limitation of the SPANI

The essential limitation of the SPANI is the need to introduce ϵ. Due to the presence of this parameter, the switch in sign of the integrator occurs later than the error switch, limiting the potential performance improvement of the SPANI.

The Filtered Split-Path Nonlinear Integrator (F-SPANI) proposed in Sec. III below introduces an additional filter with phase lead in the phase branch, which tries to "compensate" for the delay due to the presence of ϵ. The phase lead in the filter "detects" when a sign switch is approaching. Including such anticipating characteristic in the SPANI can counteract the above performance loss due to the tilting of the switching plane and, as a result can guarantee superior overall transient performance.

III. FILTERED SPLIT PATH NONLINEAR INTEGRATOR

In this section, the novel filtered SPANI (F-SPANI) design is introduced.

A. Design of the F-SPANI

The F-SPANI is schematically represented in Fig. 4, where a general filter $\mathcal{C}_f$ is included. This filter can be any filter that introduces a phase lead, such as a lead filter. Mathematically, the filter is described in state-space form by

$$\mathcal{C}_f : \begin{cases} \dot{x}_f &= A_f x_f + B_f e, \\ u_f &= C_f x_f + D_f e \end{cases} \tag{17}$$

with $x_f \in \mathbb{R}^{n_f \times 1}$ the state of the filter, and u_f the output of the filter.

B. Closed-loop Model and Stability Analysis

The inclusion of this filter adds a new state variable to the closed-loop model, but the system can still be described in the form (7a) and (7b) with adapted switching boundary $\varphi := x_I(\epsilon x_I + C_f x_f + D_f e)$. Note that tilting parameter ϵ is still needed to avoid the equilibrium x^* corresponding to $e = 0$ to be on the switching boundary.

The system matrices and states for the F-SPANI are given by

$$x = \begin{bmatrix} x_p^\top & x_c^\top & x_I & x_f^\top \end{bmatrix}^\top, \tag{18}$$

$$A_i = \begin{bmatrix} A_p - B_p D_c C_p & B_p C_c & (-1)^{i+1} B_p & 0 \\ -B_c C_p & A_c & 0 & 0 \\ -\omega_i C_p & 0 & 0 & 0 \\ -B_f C_p & 0 & 0 & A_f \end{bmatrix}, \tag{19}$$

$$B_r = \begin{bmatrix} B_p D_c \\ B_c \\ \omega_i \\ B_f \end{bmatrix} \quad B_d = \begin{bmatrix} B_p \\ 0 \\ 0 \\ 0 \end{bmatrix}, \tag{20}$$

for $i = 1, 2$ for mode 1 and 2, respectively. System matrix A_1 is assumed to be a Hurwitz matrix, which can easily be guaranteed by appropriate design of $\mathcal{C}_{\text{nom}}$, $\mathcal{C}_I$ and $\mathcal{C}_f$. Similar to the SPANI, the minus sign in the entry in the first row and third column of A_2 causes the dynamics in mode 2 to be typically unstable.

In line with the stability proof of the SPANI and using the fact that the structure in (7) of the closed-loop dynamics is the same for both the SPANI and F-SPANI, the F-SPANI can be proven to result in a globally asympotically stable closed-loop system if the same two design requirements are met for $P > 0$ and $\alpha \geq 0$, i.e.,

$$\begin{cases} A_1^\top P + P A_1 \prec 0, & \text{(21a)} \\ M^\top \left(Q(P) - \alpha R \right) M \prec 0. & \text{(21b)} \end{cases}$$

Due to the changed switching law, the matrix R is changed to (22) (on the next page), where again γ_r and γ_d are included to characterize the integrator equilibrium $x_I^* = \gamma_r r_c + \gamma_d d_c$, and ξ_r and ξ_d are introduced to characterize the filter equilibrium in $x_f^* = \xi_r r_c + \xi_d d_c$, which are defined by

$$\gamma_{r/d} = -\begin{bmatrix} O_{1\times n_p} & O_{1\times n_c} & 1 & O_{1\times n_f} \end{bmatrix} A_1^{-1} B_{r/d}, \tag{23}$$

$$\xi_{r/d} = -\begin{bmatrix} O_{n_f\times n_p} & O_{n_f\times n_c} & 0 & I_{n_f\times n_f} \end{bmatrix} A_1^{-1} B_{r/d}. \tag{24}$$

It can be shown that the kernel of R and the kernel of Q are given by the same vector

$$\ker(R) = \ker(Q) = \alpha \begin{bmatrix} O_{1\times n} & -\gamma_d & \gamma_r \end{bmatrix}^\top, \tag{25}$$

which is identical to the kernel of R and $Q(P)$ in the SPANI. Although (25) is not immediately obvious from the structure of the matrices, the relation between γ_r, γ_d, ξ_r and ξ_d warrants that (25) holds. Using this relation, the stability proof as shown for the SPANI in [15] is also valid for the F-SPANI. Hence, also an LMI-based stability check based on (21) for $P > 0$ and $\alpha \geq 0$ of the F-SPANI is supported, with an iterative search over $\epsilon \geq 0$.

IV. SIMULATION RESULTS

To illustrate the potential of the SPANI and the additional benefits of the F-SPANI, in the remainder of this paper the focus will be on an illustrative simulation example and an experimental study in Sec. V. Note that the experimental study is new for not only the F-SPANI but also for the SPANI.

For sake of illustration, a plant according to a second-order motion system is used, i.e.,

$$\mathcal{P}(s) = \frac{\omega_n^2}{s^2 + 2\beta\omega_n s + \omega_n^2} \tag{26}$$

with ω_n the eigenfrequency of the system and β the damping of the resonance peak. The specific values used in this section are chosen as $\omega_n = 3 \cdot 2\pi$ rad/s and $\beta = 0.07$.

The first step in the application of the (F-)SPANI is the design of a linear controller containing an integrator. The controller for this example is designed using loop-shaping arguments yielding

$$\mathcal{C}(s) = k \underbrace{\frac{\tau_1 s + 1}{\tau_2 s + 1}}_{\mathcal{C}_{ld}(s)} \underbrace{\frac{s + \omega_i}{s}}_{\mathcal{C}_{wi}(s)} \underbrace{\frac{1}{\tau_3 s + 1}}_{\mathcal{C}_{lp}(s)}, \tag{27}$$

where $k = 3.225$ is the gain of the filter, $\tau_1 = \frac{1}{2\pi 10/3}$ and $\tau_2 = \frac{1}{2\pi \cdot 30}$ in the lead filter $\mathcal{C}_{ld}(s)$, $\omega_i = 2\pi \cdot 10/3$ in the weak integrator $\mathcal{C}_{wi}(s)$, and $\tau_3 = \frac{1}{2\pi \cdot 80}$ in the low pass filter $\mathcal{C}_{lp}(s)$. The controller can be rewritten into a parallel structure using $\mathcal{C}_{\text{nom}}(s) = \mathcal{C}(s) - \mathcal{C}_{\text{I}}(s)$ resulting in

$$\mathcal{C}_{\text{nom}}(s) = \frac{1.452e04s + 5.644e05}{s^2 + 691.2s + 9.475e04}, \quad \mathcal{C}_{\text{I}}(s) = \frac{67.54}{s}. \tag{28}$$

The obtained bandwidth of the controller is 10 Hz. The bandwidth can easily be increased to higher frequencies, which will decrease the rise-time of the step-response significantly, however, then the overshoot of the linear controller will increase.

For the controller in (27), the step response of the closed-loop system is shown in the top figure in Fig. 5 in blue, which shows a significant overshoot of 45%. In Fig. 5, the simulation results of the SPANI with and without tilting parameter ϵ are represented by the red-dotted and yellow-dashed lines. Besides the step response, the corresponding output of the SPANI (u_s) and the sum of the absolute errors, cumulated over time, are shown. As shown in Table I, the overshoot has been reduced from 45% to 35% and 39% respectively for the SPANI with $\epsilon = 0$ and $\epsilon = 0.1616$. Additionally, the absolute cumulative error, scaled to 1 for the linear controller, has been reduced to 0.8793 and 0.8814 respectively, although the cumulative error for the SPANI with $\epsilon = 0$ is still increasing. Although the SPANI with $\epsilon \neq 0$ results in a decreased performance in terms of overshoot, the middle graph shows that the SPANI with $\epsilon = 0$ switches many times and the control effort increases gradually, while the system response is approaching steady-state. This switching and gradually growing control effort results in a residual error and is likely to be unacceptable in practice. The value for the tilting parameter ϵ is found

$$R = \begin{bmatrix} O_{n_p\times n_p} & O_{n_p\times n_c} & -\frac{1}{2}C_p^\top D_f^\top & O_{n_p\times n_f} & -\frac{1}{2}\gamma_r C_p^\top D_f^\top & -\frac{1}{2}C_p^\top D_f^\top \gamma_d \\ O_{n_c\times n_p} & O_{n_c\times n_c} & O_{n_c\times 1} & O_{n_c\times n_f} & O_{n_c\times 1} & O_{n_c\times 1} \\ -\frac{1}{2}D_f C_p & O_{1\times n_c} & \epsilon & \frac{1}{2}C_f & \frac{1}{2}C_f\xi_r + \epsilon\gamma_r & \frac{1}{2}C_f\xi_d + \epsilon\gamma_d \\ O_{n_f\times n_p} & O_{n_f\times n_c} & \frac{1}{2}C_f^\top & O_{n_f\times n_f} & \frac{1}{2}C_f^\top\gamma_r & \frac{1}{2}C_f^\top\gamma_d \\ -\frac{1}{2}\gamma_r D_f C_p & O_{1\times n_c} & \epsilon\gamma_r + \frac{1}{2}\xi_r^\top C_f^\top & \frac{1}{2}\gamma_r C_f & \frac{1}{2}\gamma_r C_f\xi_r + \frac{1}{2}\xi_r^\top C_f^\top\gamma_r + \epsilon\gamma_r^2 & \frac{1}{2}\gamma_r C_f\xi_d + \frac{1}{2}\xi_r^\top C_f^\top\gamma_d + \epsilon\gamma_r\gamma_d \\ -\frac{1}{2}\gamma_d D_f C_p & O_{1\times n_c} & \epsilon\gamma_d + \frac{1}{2}\xi_d^\top C_f^\top & \frac{1}{2}\gamma_d C_f & \frac{1}{2}\gamma_d C_f\xi_r + \frac{1}{2}\xi_d^\top C_f^\top\gamma_r + \gamma_d\epsilon\gamma_r & \frac{1}{2}\gamma_d C_f\xi_d + \frac{1}{2}\xi_d^\top C_f^\top\gamma_d + \epsilon\gamma_d^2 \end{bmatrix} \tag{22}$$

	Bandwidth = 10 Hz			Bandwidth = 100 Hz		
Controller	ϵ	Over-shoot	Error	ϵ	Over-shoot	Error
Linear	-	45%	1	-	48%	1
SPANI	0	35%	0.8793	0	40%	0.7879
SPANI	0.1616	39%	0.8814	0.0012	41%	0.7979
F-SPANI	0.4295	25%	0.6613	0.0067	33%	0.7236

TABLE I: Performance overview for two different controllers in terms of overshoot and cumulative absolute error.

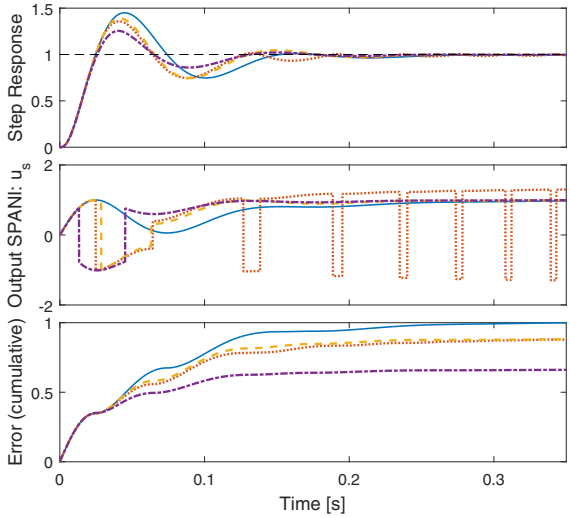

Fig. 5: Step response of the simulation example using linear control (blue) the SPANI without (red-dotted) and with (yellow-dashed) the tilting parameter and the F-SPANI (purple dash-dotted).

using a bi-section algorithm [17, Sec. 5.5], which results in the lowest feasible value for ϵ in the LMIs in (15). The stability check in [15] is slightly conservative for mode 2, which implies that smaller values of ϵ might still yield improved transient performance without oscillatory behavior. The introduction of a filter with phase lead is proposed in Sec. III in the F-SPANI to anticipate the switch of the sign of the error. In this simulation example, a lead filter

$$\mathcal{C}_f(s) = \frac{\tau_4 s + 1}{\tau_5 s + 1} \tag{29}$$

is added with $\tau_4 = \frac{1}{2\pi(10/3)}$ and $\tau_5 = \frac{1}{2\pi 30}$, which results in a phase lead of 45 degrees around the bandwidth. In Fig. 5, the results of the simulations with the F-SPANI are shown. It can be seen that the lead filter indeed results in an anticipation of the sign switch of the error. For the F-SPANI for this example, $\epsilon = 0.4295$ is found as the lowest feasible value; however, without a formal proof for

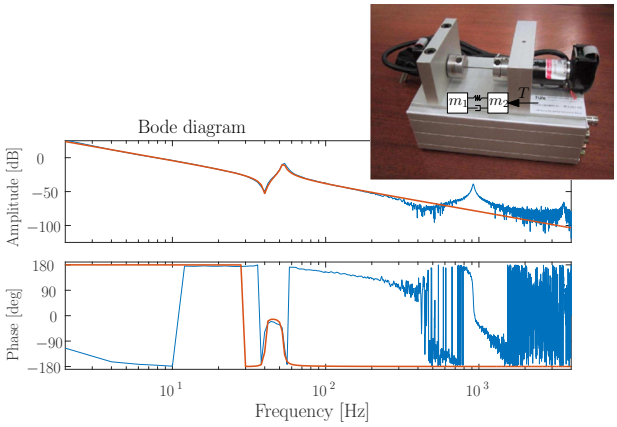

Fig. 6: Two-mass-spring-damper system, as used for the experimental validation, including the frequency response function of the system. In red a fourth-order model is fitted through the data.

stability, the tilting parameter can be reduced manually to $\epsilon = 0.17$ before unstable or switching behavior was observed in simulation. As shown in Table I, the F-SPANI has only 25% overshoot and the sum of the absolute errors over time has reduced to 0.6613. Only two switches are observed in the F-SPANI and the overshoot and settling time have reduced significantly, which shows that this method indeed improves transient performance.

For illustrative purposes, Table I shows that the relative performance improvement is unrelated to the performance of the controller. In this table, the overshoot and normalized cumulative absolute error are shown for a controller with a bandwidth of 10 Hz and of 100 Hz.

V. EXPERIMENTAL RESULTS

In this section, the SPANI including the tilting parameter and the F-SPANI with a lead filter as in (29) are compared to the linear controller in a practical application. The setup under consideration is a two-mass-spring damper system, as shown in Fig. 6. This setup can be modeled as a fourth-order motion system. To design a controller for this system, a frequency response function (FRF) of the plant dynamics is identified experimentally, as shown in Fig. 6. A fourth-order model has been fitted through the data, which is also included in the graph. It should be noted that a second resonance peak is present in the data around 920 Hz; however, this is not included in the model (the controller is assumed to be robust against such high-frequency model uncertainties). The controller is designed for a bandwidth of around 3 Hz. As such, the second resonance peak is not relevant and is

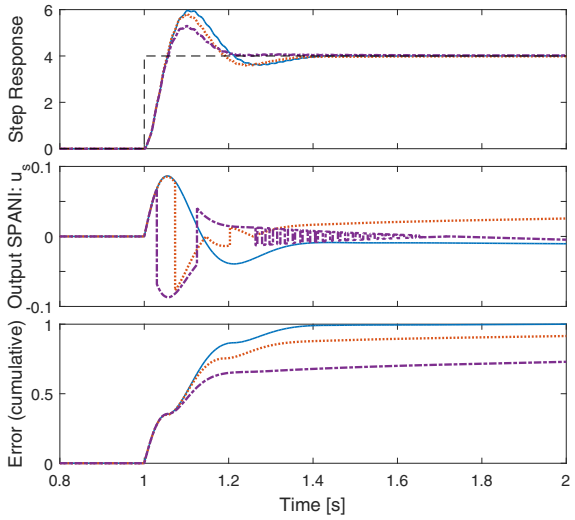

Fig. 7: Experimental results using a linear controller (blue-solid), the SPANI (red-dotted) and F-SPANI (purple dash-dotted) with a tilting parameter.

therefore not included in the model. The designed controller is given by

$$\mathcal{C}(s) = k \underbrace{\frac{\tau_1 s + 1}{\tau_2 s + 1}}_{\mathcal{C}_{ld}(s)} \underbrace{\frac{s + \tau_3}{s}}_{\mathcal{C}_{wi}(s)} \tag{30}$$

with $k = 0.083$ the gain, $\tau_1 = \frac{1}{2\pi(4/3)}$ and $\tau_2 = \frac{1}{2\pi 12}$ the zero and pole of the lead filter $\mathcal{C}_{ld}(s)$ and $\tau_3 = \frac{1}{2\pi(4/3)}$ the zero of the weak integrator $\mathcal{C}_{wi}(s)$. The resulting integrator in the parallel structure for the SPANI is given by

$$\mathcal{C}_{\text{i}}(s) = \frac{\omega_i}{s} \qquad \text{with} \quad \omega_i = 0.3267 \tag{31}$$

and $\mathcal{C}_f$ as in (29) with $\tau_4 = \frac{1}{2\pi}$ and $\tau_5 = \frac{1}{2\pi \cdot 9}$. Using the same methodology as for the simulations, the results in Fig. 7 are obtained. The values for ϵ are significantly higher than for the simulation example with $\epsilon = 14.6241$ for the SPANI and $\epsilon = 9.8506$ for the F-SPANI, however, these are the lowest feasible values for which the design requirements in (21) are satisfied. Nevertheless, the results are promising. Namely, with these values, the linear controller has an overshoot of 49%, the SPANI of 45% and the F-SPANI of 32%, which is a significant improvement of the transient performance. The middle figure shows that the F-SPANI does have some switching around the equilibrium, however, this reduces rapidly and stops 0.7 seconds after the step. A reason for this behavior might be due to the lightly damped resonance peak at 58 Hz, see Fig. 6, resulting in oscillations around $e = 0$ even for the linear controller. The absolute cumulative errors are, respectively, 1 (due to normalization), 0.9148 and 0.7294 for the linear controller, SPANI and F-SPANI respectively, which is again a significant improvement. With this experiment, it has been shown that the SPANI and the proposed F-SPANI can provide significant improvement in transient performance.

VI. CONCLUSIONS

The aim of this paper was to improve the transient performance of motion systems by means of hybrid control. The work is based on the Split-Path Nonlinear Integrator (SPANI), introduced in [14] and the SPAN filter [13]. The Filtered Split-Path Nonlinear Integrator (F-SPANI) is proposed, where overshoot is anticipated using phase lead in an additional filter included in the phase path of the SPANI design. It is shown that the stability results provided for the SPANI can be generalized towards the F-SPANI. Moreover, we demonstrated both in simulations and experiments that the proposed method indeed results in a significant improvement in transient performance. In future work, it is of interest to consider the optimization of the design of the filter $\mathcal{C}_f$ for a further increase in transient performance.

REFERENCES

[1] J. Freudenberg, R. Middleton, and A. Stefanpoulou, "A Survey of Inherent Design Limitations," in *Proceedings of the American Control Conference*, vol. 5, 2000, pp. 2987 – 3001.

[2] M. Seron, J. Braslavsky, and G. Goodwin, *Fundamental Limitations in Filterint and Control*. Berlin: Springer, 1997.

[3] G. F. Franklin, J. D. Powell, and A. Emami-Naeini, *Feedback Control of Dynamic Systems*, 5th ed. Upper Saddle River, New Jersey, USA: Pearson Education, Inc., 2006.

[4] A. Feuer, G. Goodwin, and M. Salgado, "Potential Benefits of Hybrid Control for Linear Time Invariant Plants," in *Proceedings of the American Control Conference*, 1997, pp. 2790–2794.

[5] J. C. Clegg, "A nonlinear integrator for servomechanisms," *Transactions of the American Institute of Electrical Engineers*, vol. 77, no. II, pp. 41–42, 1958.

[6] S. van Loon, K. Gruntjens, M. Heertjes, N. van de Wouw, and W. Heemels, "Frequency-domain tools for stability analysis of reset control systems," *Automatica*, 2016.

[7] W. Aangenent, G. Witvoet, W. Heemels, M. van de Molengraft, and M. Steinbuch, "Performance analysis of reset control systems," *International Journal of Robust and Nonlinear Control*, vol. 20, no. 11, pp. 1213–1233, 2009.

[8] D. Nešić, A. R. Teel, and L. Zaccarian, "Stability and performance of SISO control systems with first-order reset elements," *IEEE Transactions on Automatic Control*, vol. 56, no. 11, pp. 2567–2582, 2011.

[9] Y. Zheng, Y. Chait, C. Hollot, M. Steinbuch, and M. Norg, "Experimental demonstration of reset control design," *Control Engineering Practice*, vol. 8, pp. 113–120, 2000.

[10] B. Hunnekens, N. van de Wouw, and D. Nesic, "Overcoming a fundamental time-domain performance limitation by nonlinear control," *Automatica*, vol. 67, pp. 277–281, 2016.

[11] B. Hunnekens, N. van de Wouw, M. Heertjes, and H. Nijmeijer, "Synthesis of Variable Gain Integral Controllers for Linear Motion Systems," *IEEE Transactions on Control Systems Technology*, vol. 23, no. 1, pp. 139–149, 2015.

[12] M. F. Heertjes and Y. Vardar, "Self-tuning in Sliding Mode Control of High-Precision Motion Systems," in *Proceedings of the 6th IFAC Symposium on Mechatronic Systems*, Hangzhou, China, 2013, pp. 13–19.

[13] W. Foster, D. Gieseking, and W. Waymeyer, "A Nonlinear Filter for Independent Gain and Phase (With Applications)," *Transactions of the ASME Journal of Basic Engineering*, vol. 78, pp. 457–462, 1966.

[14] S. van Loon, B. Hunnekens, W. Heemels, N. van de Wouw, and H. Nijmeijer, "Split-path nonlinear integral control for transient performance improvement," *Automatica*, vol. 66, pp. 262–270, 2016.

[15] S. van Loon, B. Hunnekens, W. Heemels, N. van de Wouw, and H. Nijmeijer, "Transient performance improvement of linear systems using a split-path nonlinear integrator," Eindhoven University of Technology, Tech. Rep., 2014.

[16] A. Filippov, *Differential equations with discontinuous righthand sides*, ser. Mathemtaics and its applications, Eds. Dordrecht, the Netherlands: Kluwer, 1988.

[17] M. T. Heath, *Scientific Computing: An Introductory Survey*, 2nd ed. Singapore: McGraw Hill, 2005.